LETTERS

Mesoscale conformational changes in the DNA-repair complex Rad50/Mre11/Nbs1 upon binding DNA

Fernando Moreno-Herrero[1], Martijn de Jager[2], Nynke H. Dekker[1], Roland Kanaar[2,3], Claire Wyman[2,3] & Cees Dekker[1]

The human Rad50/Mre11/Nbs1 complex (hR/M/N) functions as an essential guardian of genome integrity by directing the proper processing of DNA ends, including DNA breaks[1]. This biological function results from its ability to tether broken DNA molecules[2,3]. hR/M/N's dynamic molecular architecture consists of a globular DNA-binding domain from which two 50-nm-long coiled coils protrude. The coiled coils are flexible[4] and their apices can self-associate[5]. The flexibility of the coiled coils allows their apices to adopt an orientation favourable for interaction. However, this also allows interaction between the tips of two coiled coils within the same complex, which competes with and frustrates the intercomplex interaction required for DNA tethering. Here we show that the dynamic architecture of hR/M/N is markedly affected by DNA binding. DNA binding by the hR/M/N globular domain leads to parallel orientation of the coiled coils; this prevents intracomplex interactions and favours intercomplex associations needed for DNA tethering. The hR/M/N complex thus is an example of a biological nanomachine in which binding to its ligand, in this case DNA, affects the functional conformation of a domain located 50 nm distant.

The hR/M/N complex has essential functions in various aspects of genome metabolism that involve the processing of DNA ends, such as homologous recombination, non-homologous end joining and maintenance of telomere length[1]. The molecular mechanism underlying these biological functions of hR/M/N involves tethering DNA molecules by means of the interaction between DNA-bound hR/M oligomers[2,3]. The hR/M complex is a heterotetramer, R_2M_2, arranged with a globular DNA-binding domain, including the Mre11 dimer and the two Rad50 ATPase domains, from which the long intramolecular coiled coils of Rad50 protrude[2,6,7]. The coiled-coil apex contains a CXXC amino-acid motif that forms a structure described as a zinc hook. Genetic experiments in *Saccharomyces cerevisiae* have shown that the zinc hook is an important determinant of Rad50 function[3]. Two CXXC motifs can dimerize by the coordination of a Zn^{2+} ion, providing a possible interface for interaction between hR/M complexes[5]. hR/M complexes form oligomers on linear DNA where interactions between the apices of the coiled coils then tether DNA molecules[8]. Conformational changes that alter the orientation, flexibility or dynamics of the coiled coils could be exploited to control intercomplex versus intracomplex interaction of the coiled-coil apices and therefore the biological function of hR/M. Here we resolve this issue by determining the influence of nucleotide cofactor and DNA binding on the architectural dynamics of hR/M and hR/M/N by using time-resolved atomic force microscopy (AFM) in solution.

DNA tethering requires only the hR/M complex *in vitro*. We therefore first analysed the dynamic architecture of this form, which is relevant for activity. The hR/M complex globular domain was 6.4 ± 1.0 nm high, and the coiled coils were 50 ± 3 nm long and 2.0 ± 0.3 nm high in buffer ($n = 30$) (see Fig. 1). In these high-resolution images of hR/M complexes, two, three and sometimes four individual domains could be resolved inside the globular part of the protein (Fig. 1Ce, f). These are likely to be the separate Mre11 molecules and Rad50 ATPase domains. The coiled coils of individual hR/M complexes adopted either an open conformation in which the apices of the coiled coils did not touch each other (Fig. 1A) or a closed conformation in which the apices of the coiled coils were in contact (Fig. 1B)[2,9]. In the closed conformation, the junction of the coiled coils was notably higher, 3.9 ± 0.5 nm, than that of an individual coiled coil. Single complexes frequently switched between open and

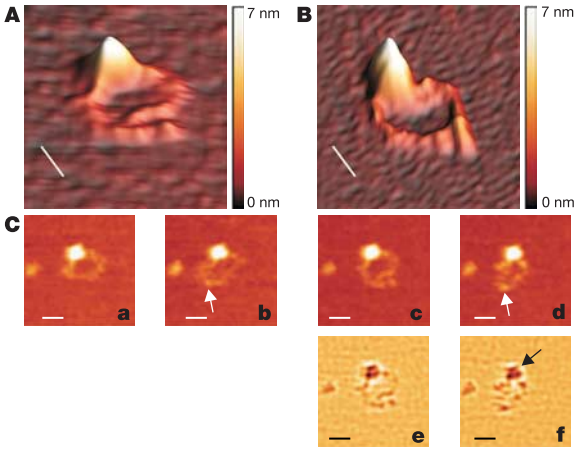

Figure 1 | Time-resolved high-resolution AFM images of the hR/M complex in buffer. A, **B**, From the globular domain, two coiled coils extend that are either not connected (open conformation, **A**) or overlapping near the apices (closed conformation, **B**). **C**, Opening and closing of the coiled coils is a dynamic process, as can be seen in the four-image sequence extracted from a movie (39 s per frame) of 13 min (**a**–**d**). The closed coiled-coils conformation is very often associated with the presence of a distinct point at the coiled-coil junction (white arrows). The frames in **e** and **f** are height images filtered with a laplacian operator to enhance substructure details. Two, three and occasionally four separate areas can be resolved inside the globular domain of hR/M (black arrow). Scale bars, 25 nm.

[1]Kavli Institute of Nanoscience, Delft University of Technology, Lorentzweg 1, 2628 CJ Delft, The Netherlands. [2]Department of Cell Biology and Genetics and [3]Department of Radiation Oncology, Erasmus MC, PO Box 1738, 3000 DR Rotterdam, The Netherlands.

closed conformations as a function of time. In Fig. 1Ca–d, four consecutive images (39 s per image) show two switches between open and closed conformations (see also Supplementary Movie 1). The interaction between the apices of the coiled coils was not primarily due to disulphide bridges between exposed cystine residues, because the addition of 2 mM dithiothreitol (DTT) to the imaging buffer did not affect the proportion of complexes with the closed conformation (48% ($n = 232$) and 45% ($n = 50$) with and without DTT, respectively).

The orientation of the hR/M coiled coils was determined in the presence and absence of the non-hydrolysable ATP analogue β-γ-imidoadenosine 5′-phosphate (AMP-PNP) and Mg^{2+}. This was quantified by measuring the angle α between the coiled coils and the longitudinal axis of the complex (see Fig. 2a). In addition, a value d for the distance between the coiled coils at the junction with the globular domain was measured (Fig. 2a). The standard deviation of the distribution of α for each molecule, displayed as error bars in Fig. 2b, provides information on the degree of mobility of the coiled coils. Molecules were analysed in three conditions (Fig. 2b): in the absence of nucleotide cofactor (black circles); after incubation with AMP-PNP but imaged in a buffer without AMP-PNP (green squares); and after incubation with AMP-PNP and imaged in the presence of AMP-PNP (blue triangles). The mean values for α obtained under these three conditions were 27 ± 8°, 26 ± 9° and 24 ± 8°, respectively, indicating that nucleotide cofactor binding does not influence the orientation or the flexibility of the coiled coils. This was unexpected, given that binding AMP-PNP causes a 30° rotation of the amino-terminal domain with respect to the carboxy-terminal domain of the *Pyrococcus furiosus* Rad50 ATPase and that the coiled coils connect these two domains[6]. If the same conformational change occurs within the ATPase domain of hRad50 after nucleotide cofactor binding, it is apparently not transmitted to the attached coiled coils. There was no correlation of the value of α with the conformation of the coiled coils: for the open conformation α was 24 ± 8° (52%, or 120 of 232), for the closed conformation α was 27 ± 8° (48%, or 112 of 232). Correspondingly, the mean value for d, 14 ± 3 nm, did not vary significantly between the molecules in the three conditions used (Fig. 2c).

Binding of hR/M to DNA induced a strikingly different arrangement of the coiled coils compared with unbound hR/M complexes. When bound to DNA by means of the globular domain, both coiled coils of the complex were parallel and on the same side of the DNA. Figure 3A shows a gallery of images of hR/M complexes bound to circular DNA in which most hR/M (93%, $n = 15$) had the architecture described above. The conformational change in hR/M was also clear in the presence of 90-base-pair (bp) linear DNA (87% parallel conformation, $n = 44$) (Fig. 3B). Movies of DNA-bound hR/M complexes showed that the coiled coils retain some flexibility and that they move synchronously. The characteristic high point located at the junction of the coiled coils (Fig. 1B) was not observed for any of the hR/M complexes bound to DNA, indicating that within a DNA-bound complex the apices of the coiled coils do not overlap. For the DNA-bound complexes, the mean angle α was 6 ± 5° (Fig. 3Da) and the mean distance d was 8 ± 3 nm. Thus, α is much smaller than the 26 ± 9° found for DNA-free hR/M. The strong effect of DNA binding on coiled-coil orientation is summarized in the histogram of the distributions of α for DNA-bound and DNA-unbound hR/M (Fig. 3Db). The presence of AMP-PNP and Mg^{2+} did not change the architecture of DNA-bound hR/M (Fig. 3C).

Time-resolved imaging in buffer also revealed the dynamic transition between the architecture of DNA-bound hR/M and the architecture of DNA-free hR/M. Figure 3Fa–f shows part of a longer movie (Supplementary Movie 2) in which, first, an hR/M complex was bound to DNA (for 8 min) and then, between the third and fourth frames, it dissociated from the DNA. Simultaneously, it changed from the parallel to the bent, open and apices-joined conformation (Fig. 3Fc, d shows the key transition frames, enlarged in Fig. 3E, G). On several occasions, the hR/M complexes were observed to move along the DNA while following the contour of the DNA molecule (Supplementary Fig. 1). This shows that hR/M can slide along DNA rather than transfer between different DNA segments. Oligomers of hR/M form only on linear DNA but are not always found at DNA ends[10]. This sliding mechanism could therefore serve to clear DNA ends for further repair processing.

The hR/M complex can also include a third subunit, Nbs1. The Nbs1 component probably interacts with the globular domain of the R/M complex and functions in signalling the presence of DNA breaks to the cell cycle checkpoint machinery[11]. The three-component complex hR/M/N appeared very similar to hR/M in our AFM study (Fig. 4a). The presence of the third subunit was evident as a larger globular domain with an average height of 8.0 ± 0.8 nm (Fig. 4b). In the absence of DNA, the hR/M/N complex also had bent, open coiled coils with apices in open and closed conformations. After DNA binding, in the presence of a molar excess of a 90-bp oligonucleotide, the coiled coils of hR/M/N also adopted a parallel conformation (86%, $n = 85$; Fig. 4c, d). The use of short DNA oligonucleotides for binding prevented the occurrence of large hR/M/N oligomers and thus allowed us to observe single intercomplex interactions through the apices of the coiled coils. Indeed, as shown in Fig. 4e, the intercomplex interaction of coiled-coil apices necessary for tethering was occasionally observed in these conditions (about 10% of the complexes observed). We never observed such an

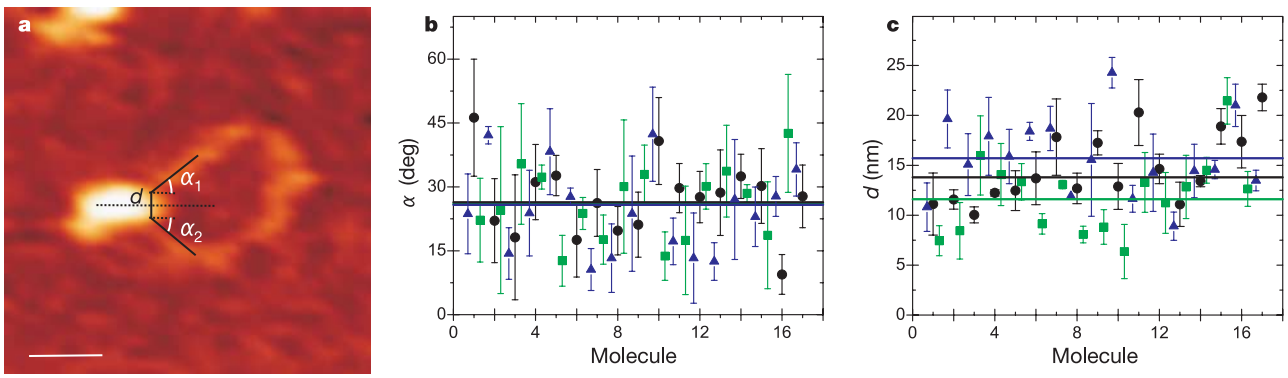

Figure 2 | Effect of nucleotide cofactor binding on the orientation of hR/M coiled coils. a, Definition of angle α ($= (\alpha_1 + \alpha_2)/2$) and distance d. Movies composed of 6–20 frames were acquired for 17 different hR/M molecules. **b**, **c**, Values (means ± s.d.) of α and d obtained for each molecule. Black circles show the results for hR/M in the absence of AMP-PNP; green squares show the results when the hR/M complex was incubated for 15 min in the presence of 2 mM $MgCl_2$ and 2 mM AMP-PNP; blue triangles show the results when, after a similar incubation, 2 mM AMP-PNP was also present in the imaging buffer.

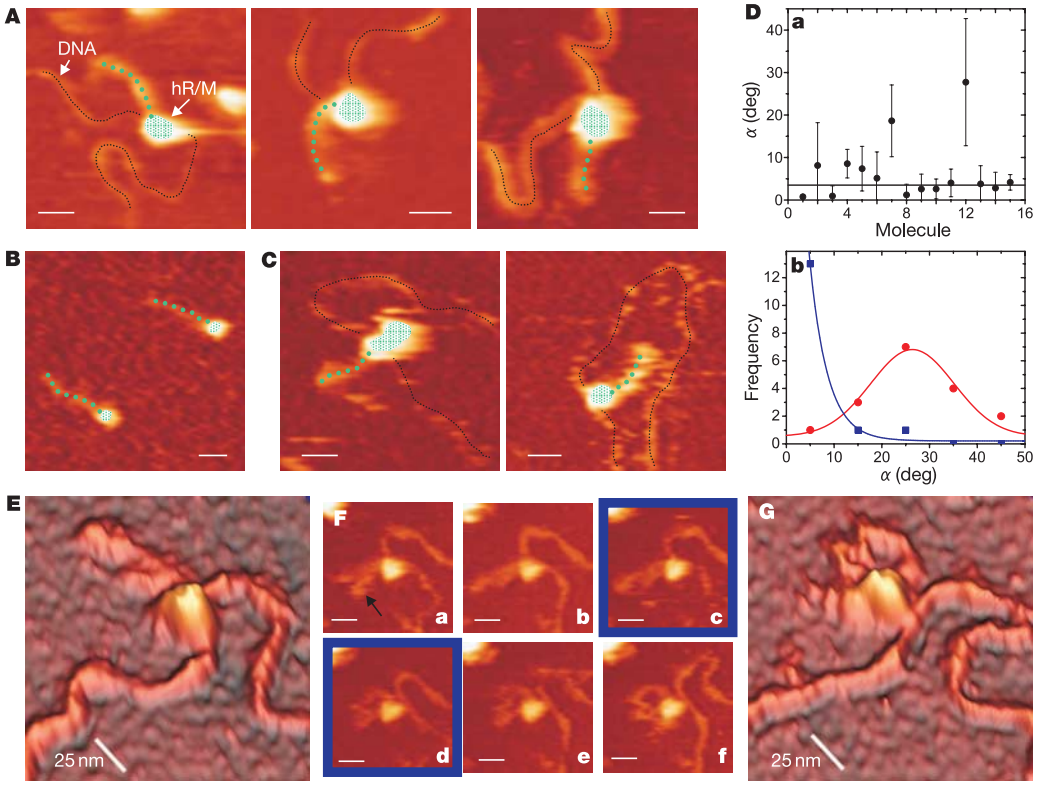

Figure 3 | hR/M binding to DNA induces a parallel alignment of the coiled coils. **A**, **B**, AFM images of hR/M complexes bound to circular double-stranded DNA (dsDNA) (**A**) and incubated with a threefold to sixfold molar excess of a 90-bp linear dsDNA (**B**). The positions of DNA and hR/M are indicated, to guide the eye. A single, thick, coiled coil protrudes from the hR/M globular domain that is bound to the DNA. **C**, A similar result was obtained when AMP-PNP was present in the binding reaction. **D**, Values (means ± s.d.) of angle α for DNA-bound hR/M (**a**) and histogram of the distributions of α for DNA-bound (blue curve) and DNA-free (red curve) hR/M (**b**). Solid lines are fits to the data. **F**, **a**–**f**, Six consecutive images extracted from a movie (39 s per frame) showing the dynamic transition from DNA-bound to free hR/M. Occasionally, the apices of the coiled coils separate from each other (black arrow). The transition frames (**c** and **d**) are highlighted and displayed in a three-dimensional rendering in **E** and **G**, enlarged and rotated through 60°. Scale bars, 30 nm unless otherwise labelled.

intercomplex configuration for hR/M and hR/M/N in the absence of DNA.

The existing molecular picture of hR/M/N function involves three processes: first, binding of the complex to DNA ends; second, the formation of large DNA-bound oligomers with the Rad50 apices of the coiled coils protruding; and third, subsequent interaction between the coiled coils of hR/M/N complexes bound to different DNA ends, to tether them and keep them close in nuclear space[8,11]. Interaction between the apices of the coiled coils is therefore essential for R/M/N function[3]. A conundrum of this molecular description centres on the control of this interaction. A single hR/M/N complex has two such apices in high local concentration. Because of the flexibility of the Rad50 coiled coils these can, and do, interact. DNA-bound hR/M/N oligomers also have many apices in high local concentration, and interaction between those bound to the same DNA molecule would be futile for tethering independent DNA ends.

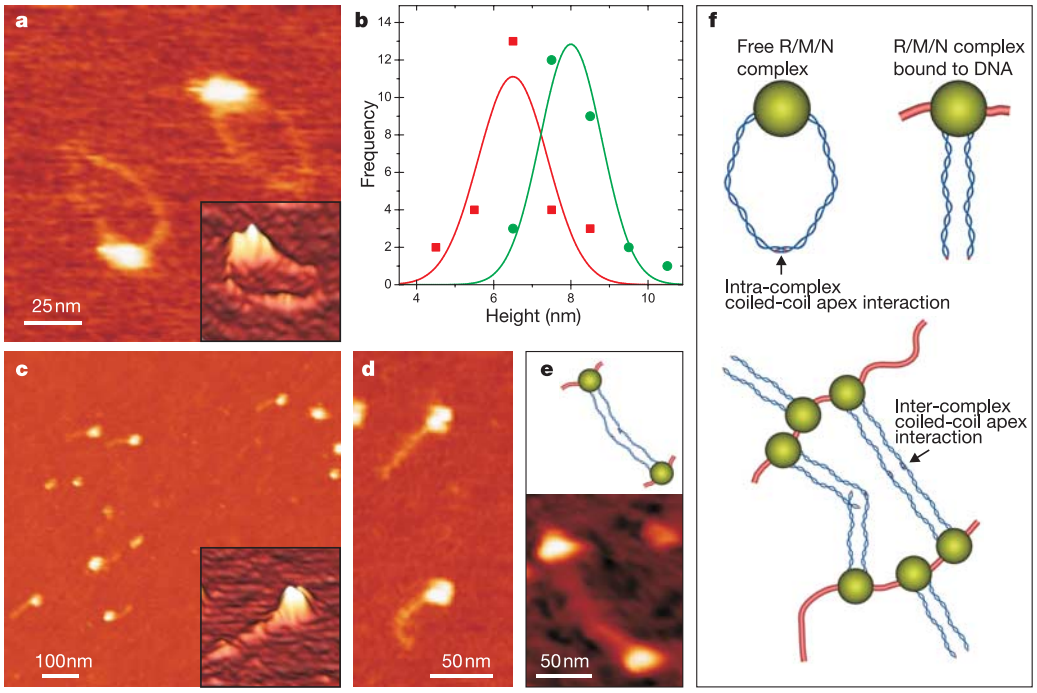

Figure 4 | Mesoscale conformational change in hR/M/N upon DNA binding and its implications for DNA-end tethering. **a**, AFM images of free hR/M/N show an architecture similar to that of hR/M. **b**, Histogram of heights for hR/M/N (green) and hR/M (red) globular domains. Solid lines are fits to the data. **c**, In the presence of a molar excess of 90-bp dsDNA, 87% of hR/M/N complexes showed a single, thick coiled coil. Insets in **a** and **c** show three-dimensional renderings of free and DNA-bound hR/M/N complexes. **d**, Detailed image showing the striking architecture of DNA-bound hR/M/N. **e**, Example of intercomplex coiled-coil apex interactions. **f**, Diagram showing the importance of conformational changes in the hR/M or hR/M/N coiled coils for DNA-end tethering.

Here we have shown that this futile intracomplex joining of Rad50 coiled-coil apices is prevented once DNA is engaged. The hR/M/N coiled coils become oriented in such a way that intracomplex interactions are prevented, while at the same time intercomplex interactions needed for tethering are favoured (Fig. 4f).

METHODS

Protein preparation. hR/M and hR/M/N were purified as described[2]. Stock solutions (1 $\mu g\,\mu l^{-1}$ in 150 mM KCl, 2 mM DTT, 25 mM Tris-HCl pH 8.0, 10% glycerol) were divided into aliquots and stored at −80 °C. A fresh aliquot was used for each AFM experiment.

DNA. pGEM-3Z plasmid (2,743 bp) was relaxed by using the nicking enzyme N.BstNB I (New England Biolabs). The isolated product was checked by gel electrophoresis and AFM inspection. A DNA fragment of 90 bp and four nucleotide overhangs was generated by annealing two complementary 94-mers, checked by gel electrophoresis and isolated with a DNA purification kit (MoBio Laboratories).

AFM sample preparation. For each experiment a protein aliquot was thawed, diluted 1:50 in storage buffer and kept on ice. A 20 µl portion of the diluted solution (400 ng of protein complex in 150 mM KCl, 25 mM Tris-HCl pH 8.0, 10% glycerol) was placed on a freshly cleaved mica disc held inside the liquid cell. After 2 min the liquid cell was filled with 1 ml of imaging buffer (3 mM $MgCl_2$, 75 mM KCl, 25 mM Tris-HCl pH 8.0). The sample was never allowed to dry. Imaging buffer conditions were carefully optimized to allow movement of the molecules on the surface while maintaining the best possible image quality. The use of large volumes of imaging buffer minimized any variation in potassium and magnesium concentrations due to evaporation. To study the effect of nucleotide cofactor on the conformation of the coiled coils, the protein complex was incubated for 15 min at room temperature (~22 °C) in 150 mM KCl, 25 mM Tris-HCl pH 8.0, 10% glycerol, containing 2 mM AMP-PNP and 2 mM $MgCl_2$. Subsequent sample preparation proceeded as described above.

DNA binding reaction. hR/M DNA binding reactions included 10 ng of circular DNA and 100 ng of hR/M in 15 mM $MgCl_2$, 75 mM KCl, 15 mM Tris-HCl pH 8.0, 5% glycerol in a total volume of 10 µl. The binding reaction was performed for 15 min at room temperature. The whole reaction mixture was deposited on a mica disc and imaging was done in 1 ml of imaging buffer supplemented with 2 nM hR/M. hR/M and hR/M/N were mixed with the 90-bp oligonucleotide in the same conditions with a twofold to eightfold molar excess of DNA over protein.

AFM imaging. hR/M and hR/M/N DNA binding reactions were performed in solution before the sample was deposited on a mica surface. Biological particles were partly immobilized on mica by carefully tuning the AFM imaging conditions to allow the detection of movement. Samples were imaged in buffer with a commercial AFM from Nanotec Electronica operating in tapping mode, using Olympus cantilevers (0.05 N m^{-1}, Olympus TR400 PSA). Typical tapping amplitudes at imaging were 5–7 nm at the resonance frequency of the cantilevers in liquids (9.5–10.5 kHz). Images were acquired at rates of 30 s per image (128 pixels, 500 nm) and 60 s per image (256 pixels, 1,000 nm). Imaging was always from left to right (fast scan direction) and from up to down (slow scanning direction), to minimize any piezo creep effects. The absence of any correlation between the scanning direction and the orientation of the hR/M coiled coils as well as the observation of objects moving in the direction opposite to scanning indicate that the observed dynamics were not dominated by interaction of the scanning tip with the sample.

Image processing and measurements. Image processing was performed with WSxM software (www.nanotec.es). Standard image processing consisted of plane subtraction and flattening. To capture dynamic events, consecutive images were taken at the same spot. These images were aligned by using cross-correlation filters and shown sequentially to build up a movie. By checking consecutive frames it was possible to observe which parts of the hR/M complex or which areas of DNA were mobile and loosely bound to the mica surface. The measurement of the angle between hR/M coiled coils was done by manually tracing the direction of both coiled coils in the vicinity of the globular domain. The contact of the traced line with the globular domain defines a segmented line with two angles, α_1 and α_2, and a distance d. α is defined as the arithmetic mean of α_1 and α_2.

Received 21 January; accepted 19 June 2005.

1. Connelly, J. C. & Leach, D. R. Tethering on the brink: the evolutionarily conserved Mre11–Rad50 complex. *Trends Biochem. Sci.* **27,** 410–418 (2002).
2. de Jager, M. *et al.* Human Rad50/Mre11 is a flexible complex that can tether DNA ends. *Mol. Cell* **8,** 1129–1135 (2001).
3. Wiltzius, J. J. W., Hohl, M., Fleming, J. C. & Petrini, J. H. J. The Rad50 hook domain is a critical determinant of Mre11 complex functions. *Nature Struct. Mol. Biol.* **12,** 403–407 (2005).
4. van Noort, J. *et al.* The coiled-coil of the human Rad50 DNA repair protein contains specific segments of increased flexibility. *Proc. Natl Acad. Sci. USA* **100,** 7581–7586 (2003).
5. Hopfner, K. P. *et al.* The Rad50 zinc-hook is a structure joining Mre11 complexes in DNA recombination and repair. *Nature* **418,** 562–566 (2002).
6. Hopfner, K. P. *et al.* Structural biology of Rad50 ATPase: ATP-driven conformational control in DNA double-strand break repair and the ABC-ATPase superfamily. *Cell* **101,** 789–800 (2000).
7. Hopfner, K. P. *et al.* Structural biochemistry and interaction architecture of the DNA double-strand break repair Mre11 nuclease and Rad50 ATPase. *Cell* **105,** 473–485 (2001).
8. Wyman, C. & Kanaar, R. Chromosome organization: reaching out to embrace new models. *Curr. Biol.* **12,** R446–R448 (2002).
9. de Jager, M. *et al.* Differential arrangements of conserved building blocks among homologs of the Rad50/Mre11 DNA repair protein complex. *J. Mol. Biol.* **339,** 937–949 (2004).
10. de Jager, M. *et al.* DNA-binding and strand-annealing activities of human Mre11: implications for its roles in DNA double-strand break repair pathways. *Nucleic Acids Res.* **29,** 1317–1325 (2001).
11. Stracker, T. H., Theunissen, J. W., Morales, M. & Petrini, J. H. J. The Mre11 complex and the metabolism of chromosome breaks: the importance of communicating and holding things together. *DNA Repair (Amst.)* **3,** 845–854 (2004).

Supplementary Information is linked to the online version of the paper at www.nature.com/nature.

Acknowledgements We thank T. Paull for the gift of the baculoviruses producing hRad50, hMre11 and hNbs1, and R. Seidel for useful discussions. F.M.-H. is supported by a postdoctoral fellowship from La Fundación Ramón Areces. M.d.J. is supported by an EUR fellowship from the Erasmus MC. This project is supported in part by a grant from NWO-FOM/ALW (Netherlands Organization for Scientific Research) to R.K., C.W. and C.D. Work in the laboratories of R.K. and C.W. is supported by grants from the European Commission, NWO and the Dutch Cancer Society. Work in the laboratory of C.D. and N.D. acknowledges support from FOM and NWO.

Author Information Reprints and permissions information is available at npg.nature.com/reprintsandpermissions. The authors declare no competing financial interests. Correspondence and requests for materials should be addressed to C.D. (dekker@mb.tn.tudelft.nl) and C.W. (c.wyman@erasmusmc.nl).